MIKE 21 Flow Model

Mud Transport Module

Scientific Documentation

PLEASE NOTE

COPYRIGHT

This document refers to proprietary computer software which is pro-tected by copyright. All rights are reserved. Copying or other repro-duction of this manual or the related programs is prohibited without prior written consent of DHI A/S (hereinafter referred to as "DHI"). For details please refer to your 'DHI Software Licence Agreement'.

LIMITED LIABILITY

The liability of DHI is limited as specified in your DHI Software Licence Agreement:

In no event shall DHI or its representatives (agents and suppliers) be liable for any damages whatsoever including, without limitation, special, indirect, incidental or consequential damages or damages for loss of business profits or savings, business interruption, loss of business information or other pecuniary loss arising in connection with the Agreement, e.g. out of Licensee's use of or the inability to use the Software, even if DHI has been advised of the possibility of such damages.

This limitation shall apply to claims of personal injury to the extent permitted by law. Some jurisdictions do not allow the exclusion or limitation of liability for consequential, special, indirect, incidental damages and, accordingly, some portions of these limitations may not apply.

Notwithstanding the above, DHI's total liability (whether in contract, tort, including negligence, or otherwise) under or in connection with the Agreement shall in aggregate during the term not exceed the lesser of EUR 10.000 or the fees paid by Licensee under the Agree-ment during the 12 months' period previous to the event giving rise to a claim.

Licensee acknowledge that the liability limitations and exclusions set out in the Agreement reflect the allocation of risk negotiated and agreed by the parties and that DHI would not enter into the Agree-ment without these limitations and exclusions on its liability. These limitations and exclusions will apply notwithstanding any failure of essential purpose of any limited remedy.

CONTENTS

1 Scientific Documentation

1.1 What is Mud

Mud is a term generally used for fine-grained and cohesive sediment with grain-sizes less than 63 microns. Mud is typically found in sheltered areas protected from strong wave and current activity. Examples are the upper and mid reaches of estuaries, lagoons and coastal bays. The sources of the fine-grained sediments may be both fluvial and marine.

Fine-grained suspended sediment plays an important role in the estuarine environment. Fine sediment is brought in suspension and transported by current and wave actions. In estuaries, the transport mechanisms (settling – and scour lag) acting on the fine-grained material tend to concentrate and deposit the fine-grained material in the inner sheltered parts of the area (Postma, 1967; Pejrup, 1988). A zone of high concentration suspension is called a turbidity maximum and will change its position within the estuary depending on the tidal cycle and the input of fresh-water from rivers, etc. (Dyer, 1986).

Fine sediments are characterised by slow settling velocities. Therefore, they may be transported over long distances by the water flow before settling. The cohesive properties of fine sediments allow them to stick together and form larger aggregates or flocs with settling velocities much higher than the individual particles within the floc (Krone, 1986; Burt, 1986). In this way they are able to deposit in areas where the individual fine particles would never settle. The formation and destruction of flocs are depending on the amount of sediment in suspension as well as the turbulence properties of the flow. This is in contrast to non-cohesive sediment, where the particles are transported as single grains.

Figure 1.1   Muddy (left) and sandy (right) sediments

Fine sediment is classified according to grain-size as shown in the table below.

Table 1.1   Classification of fine sediment

Sediment type	Grain size
Clay	< 4 μm
Silt	4-63 μm
Fine sand	63-125 μm

1.2   General Model Description

1.2.1   Introduction

In order to include the transport and deposition processes of fine-grained material in the modelling system, it is necessary to integrate the description with the advection-diffusion equation caused by the water flow.

MIKE 21 is a depth-integrated, two-dimensional flow model. This means that the simulation of the transport of fine-grained material must be averaged over depth and appropriate parameterisations of the sediment processes must be applied.

In the MIKE 21 model complex, the transport of fine-grained material (mud) has been included in the Mud Transport module (MT), linked to the Hydrodynamic module (HD) and the Advection-Dispersion (AD) module, as indicated in Figure 1.2.
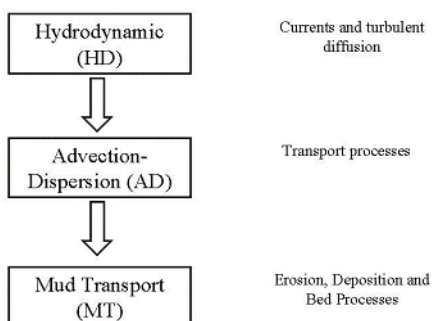

Figure 1.2   Data flow and physical processes for MIKE 21

The combination of the Multi-Fraction and Multi-Layer models is an extension compared to the earlier versions of MIKE 21 MT, where these models were independent.

The processes included in the MT module are kept as general as possible. The MT module includes the following processes:

- Multiple mud fractions
- Multiple bed layers
- Wave-current interaction
- Flocculation
- Hindered settling
- Inclusion of a sand fraction
- Sliding
- Consolidation of layers
- Simple morphological calculations

The above possibilities cover most cases appropriate for 2D modelling. In case special applications are required such as simulating the influence of high sediment concentrations on the water flow through formation of stratification and damping of turbulence, the modeller is referred to MIKE 3 MT.

1.2.2   The AD module

The sediment transport formulations are built into the advection-dispersion module, MIKE 21 AD.

MIKE 21 AD solves the so-called advection-dispersion equation:

$$\frac{\partial \bar{c}}{\partial t} + u\frac{\partial \bar{c}}{\partial x} + v\frac{\partial \bar{c}}{\partial y} =$$
$$\frac{1}{h}\frac{\partial}{\partial x}\left(hD_x\frac{\partial \bar{c}}{\partial x}\right) + \frac{1}{h}\frac{\partial}{\partial y}\left(hD_y\frac{\partial \bar{c}}{\partial y}\right) + Q_L C_L \frac{1}{h} - S \qquad (1.1)$$

Symbol List

$\bar{c}$	depth averaged mass concentration (kg/m^3)
u,v	depth averaged flow velocities (m/s)
D_x, D_y	dispersion coefficients (m^2/s)
h	water depth (m)
S	accretion/erosion term (kg/m^3/s)
Q_L	source discharge per unit horizontal area (m^3/s/m^2)
C_L	concentration of source discharge (kg/m^3)

In cases of multiple sediment fractions, the equation is extended to include several fractions while the deposition and erosion processes are connected to the number of fractions.

The advection-dispersion equation is solved using an explicit, third-order finite difference scheme, known as the ULTIMATE scheme, Leonard (1991). This scheme is based on the well-known QUICKEST scheme, Leonard (1979), Ekebjærg et al. (1991).

This scheme has been described in various papers dealing with turbulence modelling, environmental modelling and other problems involving the advection-dispersion equation. It has several advantages over other schemes, especially that it avoids the "wiggle" instability problem associated with central differentiation of the advection terms. At the same time it greatly reduces the numerical damping, which is characteristic of first-order up-winding methods.

The scheme itself is a Lax-Wendroff or Leith-like scheme in the sense that it cancels out the truncation error terms due to time differentiation up to a certain order by using the basic equation itself. In the case of QUICKEST, truncation error terms up to third-order are cancelled for both space and time derivatives.

The solution of the erosion and the deposition equations are straightforward and do not require special numerical methods.

Firstly is outlined the scientific background for the fine-grained sediment < 63 μm followed by the sand fraction.

1.3   Cohesive Sediments

1.3.1   Introduction

The mud transport module of MIKE 21 describes the erosion, transport and deposition of fine-grained material < 63 μm (silt and clay) under the action of currents and waves. For a correct solution of the erosion processes, the consolidation of sediment deposited on the bed is also included. The model is essentially based on the principles in Mehta et al. (1989) with the innovation of including the bed shear stresses due to waves.

Clay particles have a plate-like structure and an overall negative ionic charge due to broken mineral bonds on their faces. In saline water, the negative charges on the particles attract positively charged cations and a diffuse cloud of cations is formed around the particles. In this way the particles tend to repel each other (Van Olphen, 1963). Still, particles in saline water flocculate and form large aggregates or flocs in spite of the repulsive forces. This is because in saline water, the electrical double layer is compressed and the attractive van der Waals force acting upon the atom pairs in the particles

becomes active. Flocculation is governed by increasing concentration, because more particles in the water enhance meetings between individual particles. Turbulence also plays an important role for flocculation both for the forming and breaking up of flocs depending on the turbulent shear (Dyer, 1986).

A deterministic physically based description of the behaviour of cohesive sediment has not yet been developed, because the numerous forces included in their behaviour tend to complicate matters. Consequently, the mathematical descriptions of erosion and deposition are essentially empirical, although they are based on sound physical principles.

The lack of a universally applicable, physically based formulation for cohesive sediment behaviour means that any model of this phenomenon is heavily dependent on field data (Andersen & Pejrup, 2001; Andersen, 2001; Edelvang & Austen, 1997; Pejrup et al., 1997). Extensive data over the entire area to be modelled is required such as:

- bed sedimentology
- bed erodibility
- biology
- settling velocities
- suspended sediment concentrations
- current velocities
- vertical velocity and suspended sediment concentration profiles
- compaction of bed layers
- effect of wave action
- critical shear stresses for deposition and erosion

Naturally, the dynamic variation of water depth and flow velocities must also be known along with boundary values of suspended sediment concentration.

The MIKE 21 MT module consists of a 'water-column' and an 'in-the-bed' module. The link between these two modules is source/sink terms in an advection-dispersion model.

The transport and deposition of fine-grained material is governed by the fact that settling velocities are generally slow compared to sand. Hence, the concentration of suspended material does not adjust immediately to changes in the hydraulic conditions. In other words, the sediment concentration at a given time and location is dependent on the conditions upstream of this location at an earlier time. Postma (1967) first described this process, called settling- and scour-lag. This is the main factor for the concentration of fine material in estuaries often resulting in a turbidity maximum. In order to describe this process, the sediment computation has been built into the advection-dispersion module, MIKE 21 AD.

The source and sink term S in the advection-dispersion equation depends on whether the local hydrodynamic conditions cause the bed to become eroded or allow deposition to occur. Empirical relations are used, and possible formulations for evaluating S are given below.

The mobile suspended sediment is transported by long-period waves only, which are tidal currents, whereas the wind-waves are considered as "shakers". Combined they are able to re-entrain or re-suspend the deposited or consolidated sediment.

The processes in the bed are described in a multi-layer bed (max. 8); each described by a critical shear stress, erosion coefficient , power of erosion, density of dry sediment and erosion function. The bed layers can be dense and consolidated or soft and partly consolidated.

Liquefaction by waves is included as a weakening of the bed due to breakdown of the bed structure.

Consolidation is included between the layers as a transition rate of sediment between the layers.

In areas with deep channels or large variations in water depths it is possible to include a sliding process, which allows sediment to slide down to deeper areas due to gravity and current motion. This is described by a dispersion equation.

1.3.2   Model description

The physical processes are modelled by a "multi bed layer approach". An example with 3 bed layers is shown in Figure 1.3.

Processes

- flocculation
- settling
- deposition
- consolidation
- re-suspension by currents and waves
- erosion by currents and waves
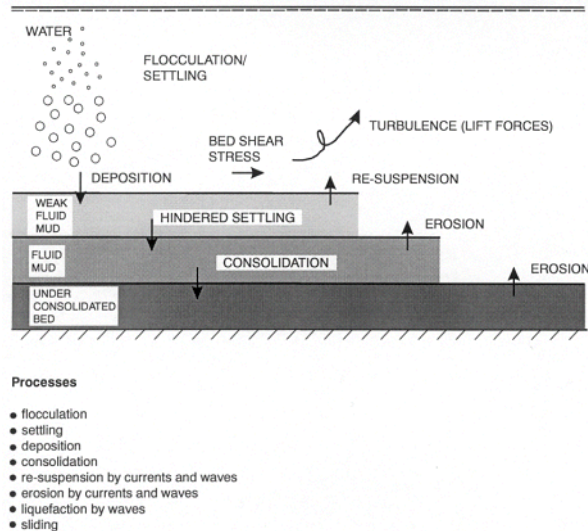- liquefaction by waves
- sliding

Figure 1.3   Multi-layer model and physical processes

1.3.3   Deposition

In the MT model, a stochastic model for flow and sediment interaction is applied. This approach was first developed by Krone (1962).

Krone suggests that the deposition rate can be expressed by

Deposition: $S_D = w_s c_b p_d$

w_s	settling velocity (m/s)
c_b	near bed concentration (kg/m^3)
p_d	probability of deposition
	$= 1 - \dfrac{\tau_b}{\tau_{cd}}, \tau_b \leq \tau_{cd}$
τ_b	the bed shear stress (N/m^2)
τ_{cd}	critical bed shear stress for deposition (N/m^2)

1.3.4   Settling velocity and flocculation

The settling velocity of the fine sediment depends on the particle/floc size, temperature, concentration of suspended matter and content of organic material.

Usually one distinguishes between a regime where the settling velocity increases with increasing concentration (flocculation) and a regime where the settling velocity decreases with increasing concentration. The latter is referred too as hindered settling. The first is the most common of the two in the estuary.

Following Rijn (1989) the settling velocity in saline water (>5 ppt) can be expressed by:

$$w_s = kc^{\gamma} \text{ for } c \leq 10 \text{ kg/m}^3 \tag{1.2}$$

where

w_s	settling velocity of flocs (m/s)
c	mass concentration
k, γ	coefficients
γ	1 to 2

The relation for $c \leq 10\text{kg/m}^3$ describes the flocculation of particles based on particle collisions. The higher concentration the higher possibility for the particles to flocculate.

$c > 10\text{kg/m}^3$ corresponds to "hindered" settling, where particles are in contact with each other and do not fall freely through the water.

Alternative settling formulations are also available:

The formulation of Richardson and Zaki (1954) is the classical equation for hindered settling.

$$w_s = w_{s,r}\left(1 - \frac{c}{c_{gel}}\right)^{w_{s,n}} \tag{1.3}$$

Where $w_{s,r}$ is a reference value, $w_{s,n}$ a coefficient and c_{gel} the concentration at which the flocs start to form a real self-supported matrix (referred to as the gel point).

Winterwerp (1999) proposed the following for hindered settling.

$$w_s = w_{s,r}\frac{(1 - \Phi_*)(1 - \Phi_p)}{1 + 2.5\Phi} \tag{1.4}$$

where

$$\Phi_p = \frac{c}{\rho_s} \tag{1.5}$$

and ρ_s is the density of sediment grains.

Flocculation is enhanced by high organic matter content including organic coatings, etc. (Van Leussen, 1988; Eisma, 1993). In fresh water, flocculation is dependent on organic matter content, whereas in saline waters salt floccu-

lation also occurs. The influence of salt on flocculation is primarily important in areas where fresh water meets salt water such as estuaries. The following expression is used to express the variation of settling velocity with salinity. Notice that the reference value ws is the value representative for saline water.

$$w_s = w_s(1 - C_1 e^{C_2})$$ (1.6)

where C_1 and C_2 are calibration parameters.

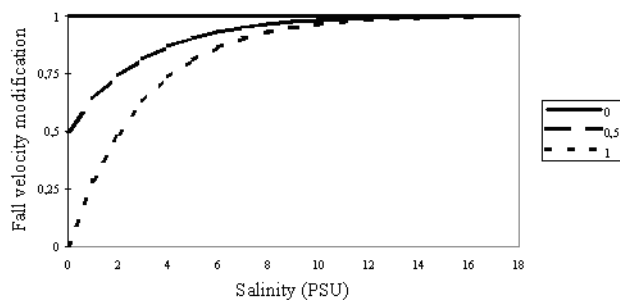Figure 1.4 shows an example of C_1 ={0 , 0.5 , 1} and C_2 = -1/3.

Figure 1.4   Settling velocity and salinity dependency

The description of salt flocculation is based on Krone's experimental research, Krone (1962). Whitehouse et al., 1960) studied the effect of varying salinities on flocculation of different clay minerals in the laboratory. Gibbs (1985) showed that in the natural environment, flocculation is more dependent on organic coating. Therefore, the effect of mineral constitution of the sediment is not taken is not account in the model. Furthermore, information on mineralogy of bed sediments is rarely available.

1.3.5   Sediment concentration profiles

Two expressions for the sediment concentration profile can be applied. Either an expression that is based on an approximate solution to the vertical sediment fluxes during deposition (Teeter) or an expression that assumes equilibrium between upward and downward sediment fluxes (Rouse).

Teeter 1986 profile

The near bed concentration c_b is proportional to the depth averaged mass concentration $\bar{c}$ and is related to the vertical transport, i.e. a ratio of the vertical convective and diffusive transport represented by the Peclet number:

$$P_e = \frac{C_{rc}}{C_{rd}}$$ (1.7)

where

C_{rc}	convective Courant number $= w_s\dfrac{\Delta t}{h}$
C_{rd}	diffusive Courant number $= \bar{D}_z\dfrac{\Delta t}{h^2}$
$\bar{D}_2$	depth mean eddy diffusivity
C_b	near bed concentration and is related to the depth averaged concentration $\bar{c}$, Teeter (1986).

$$\beta = \frac{c_b}{\bar{c}}$$ (1.8)

where

$$\beta = 1 + \frac{P_e}{1.25 + 4.75 p_d^{2.5}}$$ (1.9)

$$P_e - \text{Peclet number} = \frac{w_s h}{\bar{D}_z} = \frac{6 w_s}{\kappa U_f}$$ (1.10)

p_d	probability of deposition

Rouse profile

The suspended sediment is affected by turbulent diffusion, which results in an upward motion. This is balanced by settling of the grains. The balance between diffusion and settling can be expressed:

$$-\varepsilon\frac{dC}{dz} = wC$$ (1.11)

Symbol list

ε	diffusion coefficient
C	concentration as function of z

| z | vertical Cartesian coordinate |
| w | mean settling velocity of the sediment |

By assuming that ε is equal to the turbulent eddy viscosity, and applying the parabolic eddy viscosity distribution

$$\varepsilon = \kappa U_f z\left(1 - \frac{z}{h}\right) \tag{1.12}$$

Symbol list

| κ | Von Karman's universal constant ($\kappa = 0.4$) |
| U_f | Friction velocity |

$$U_f = \sqrt{\frac{\tau_b}{\rho}} \tag{1.13}$$

| ρ | fluid density |

The following vertical concentration profile will be given

$$C = C_a\left[\frac{a}{h-a}\frac{h-z}{z}\right]^R, a \leq z \leq h \tag{1.14}$$

Symbol list

C_a	reference concentration at z = a
a	reference level
z	distance from seabed
R	Rouse number

$$R = \frac{w}{\kappa U_f} \tag{1.15}$$

It is possible to choose a vertical variation of the concentration of suspended sediment in order to determine the settling distance. The average depth, h* through which the particles settle at deposition is given by

$$\frac{h*}{h} = \frac{\int\limits_{0}^{1} s\left(\frac{1}{s} - 1\right)^R ds}{\int\limits_{0}^{1} \left(\frac{1}{s} - 1\right)^R ds} \qquad (1.16)$$

where s = h/z. and the term $\frac{h*}{h}$ is named the relative height of centroid.

The suspended sediment concentration c_b is related to the depth-averaged concentration $\bar{c}$ using the Rouse profile

$$c_b = \frac{\bar{c}}{RC} \qquad (1.17)$$

In which RC is the relative height of centroid.

1.3.6   Erosion

Erosion can be described in two ways depending upon whether the bed is dense and consolidated or soft and partly consolidated, Mehta et al. (1989).

Dense, consolidated bed:

Erosion: $S_E = E(\tau_b / \tau_{ce} - 1)^n, \tau_b > \tau_{ce}$

where

E	erodibility of bed (kg/m^2/s)
τ_{ce}	critical bed shear stress for erosion (N/m^2)
n	power of erosion

Soft, partly consolidated bed:

Erosion: $S_E = E \exp[\alpha(\tau_b - \tau_{ce})^{1/2}], \tau_b > \tau_{ce}$

where

α	coefficient (m/N$^{1/2}$)

1.3.7   Bed description

It is possible to describe the bed as having more than one layer. Each layer is described by the critical shear stress for erosion, $\tau_{ce,j}$, power of erosion, n_j,

density of dry bed material, ρ_i, erosion coefficient, E_j, and α_j-coefficient. The deposited sediment is first included in the top layer. The layers represent weak fluid mud, fluid mud and under-consolidated bed, Mehta et al. (1989) and are associated with different time scales.

The model requires an initial thickness of each layer to be defined.

The consolidation process is described as the transition of sediment between the layers, Teisson (1992).

The influence of waves is taken into account as liquefaction resulting in a weakening of the bed due to breakdown of bed structure. This may cause increased surface erosion, because of the reduced strength of the bed top layer (Delo and Ockenden, 1992).

In areas where large bathymetry gradients are present, i.e. in navigational channels, it is possible to invoke a process describing the sliding of sediment from shallow parts into the channels. This will especially be possible in the top bed layers, where weak mud often will be present.

The initiation of the sliding process depends on the slope of the bathymetry, and the dry density of the actual bed layer, ρ_i (Unit: g/m^3), which corresponds to an equilibrium slope (α_e) of the bed. The relation is

Sliding $\qquad\qquad \alpha \geq \alpha_e$
No sliding $\qquad\qquad \alpha < \alpha_e$

where

α $\qquad\qquad$ actual slope of bathymetry

$$\alpha_e \; = \; arc\tan\left[2.5 \cdot 10^{-13}\left(\frac{\rho_i}{1000}\right)^{4.7}\right] \tag{1.18}$$

The sliding process is modelled by a dispersion equation, see Teisson (1991).

$$\frac{\partial_{zb}}{\partial t} \; = \; K_{sx}\frac{\partial^2 z_b}{\partial x^2} + K_{sy}\frac{\partial^2 z_b}{\partial y^2} \tag{1.19}$$

where

z_b $\qquad\qquad$ bed level
K_{sx}, K_{sy} $\qquad\qquad$ dispersion coefficients in x,y directions

The dispersion coefficients, K_{sx}, K_{sy} may be either constant or related to some model parameters, Grishanin and Lavygin (1987).

$$\vec{K}_s = \frac{9.8 \cdot 10^{-8}}{1-\varepsilon}\sqrt{(s-1)gd_{50}}\left(\frac{h}{d_{50}}\right)^{\frac{1}{6}}\frac{h\vec{v}}{(gv)^{\frac{2}{3}}}$$ (1.20)

where

$\vec{K}_S$	(K_{sx}, K_{sy})
ε	medium porosity factor
s	relative density of bed layer material
d_{50}	mean diameter of bed layer
h	water depth
$\vec{v}$	(V_x, V_y) - components of depth-averaged flow velocities
v	kinematic viscosity of water
g	gravity acceleration

All other parameters besides the K_{sx}, K_{sy} are explicitly calculated by the model. The lack of proper sediment characteristics (ε,s) prevents a satisfactory calibration of the sliding process.

1.4 Fine sand sediment transport

The major difference between the description of cohesive sediment transport and sand transport is the distinction of the suspended sediment concentration profile. In the mud transport module, a simple description of the vertical concentration profile is applied. The time-scale needed to deform the profile by the flow-conditions is long in comparison to a concentration profile of sand, which is primarily transported as bed-load.

However, it is possible to activate sand transport formulations in the MT module in case a certain percentage of the bed material is in the fine sand fraction between 63 and 125 μm that may be transported both in suspension and as bed load. These formulations are built into the advection-dispersion module, MIKE 21 AD.

The equilibrium concentration $\overline{c}_e$ is defined as

$$\overline{c}_e = \frac{q_s}{\overline{u}h}$$ (1.21)

Where $\overline{u}$ is the depth averaged flow velocity.

The suspended load transport is found as the integral of the current velocity profile, u, and the concentration profile of suspended sediment, c:

$$q_s = \int_a^h c \cdot u \, dy \qquad (1.22)$$

Symbol List

q_s	suspended load transport (kg/m/s)
c	concentration of sediment (kg/m^3) at distance y from bed
u	flow velocity (m/s) at distance y from bed
h	water depth (m)
a	thickness of the bed layer (m)

Normally little is known about the bed layer, such as the height of the bed forms. This results in the approximation:

$$a = k_s = 2d_{50} \qquad (1.23)$$

Symbol List

a	thickness of bed layer (m)
k_s	equivalent roughness height (m)
d_{50}	50 percent fractile of grain-size of sediment (m)

In MIKE 21 AD the suspended transport is calculated based on depth-averaged flow velocities $\bar{u}$, $\bar{v}$ a compound concentration, $\bar{c}$ and the water depth, h (approx. $h \approx$ h-a). The sand transport is described through a depth-averaged equilibrium concentration, $\bar{c}_e$ and an accretion (deposition), erosion term, S, which means that no bed transport takes place.

$$w_s = \begin{cases} \dfrac{(s-1)gd^2}{18v} & d < 100\,\mu m \\[2ex] \dfrac{10v}{d}\left\{\left[1 + \dfrac{0.01(s-1)gd^3}{v^2}\right]^{0.5} - 1\right\} & 100 < d \le 1000\,\mu m \\[2ex] 1.1\left[(s-1)gd\right]^{0.5} & d > 1000\,\mu m \end{cases} \qquad (1.24)$$

The following description is mainly based on Rijn (1982), (1984), Yalin (1972), Engelund, Fredsøe (1976).

The transport is highly dependent upon two parameters, namely the settling velocity, w_s and the turbulent sediment diffusion coefficient, ε_s, because these

parameters have an effect on both the flow velocity and concentration profile. For a normal sediment load the effect on the velocity profile is negligible.

The presence of sediment suspension demands that the actual friction velocity, U_f, is larger than a so-called critical friction velocity, $U_{f,cr}$, and that the vertical turbulence is sufficient to create vertical velocity components higher than the settling velocity.

The first assumption is expressed through the transport stage parameter, T

$$T = \begin{cases} \left(\dfrac{U_f}{U_{f,cr}}\right)^2 - 1, & U_f > U_{f,cr} \\ 0, T \le 0 & U_f \le U_{f,cr} \end{cases} \tag{1.25}$$

where $U_{f,cr}$ is found from Shields curve, see Rijn (1982), using the input parameters, d_{50}, relative density of sediment, s, and the dimensionless grain size, $d*$, defined as the cube root of the ratio of immersed weight to viscous forces

$$d* = d_{50}\left[\frac{(s-1)g}{\nu^2}\right]^{1/3} \tag{1.26}$$

where ν is the kinematic viscosity of water (m²/s).

The friction velocity, U_f, reads

$$U_f = \sqrt{ghI} = \frac{\sqrt{g}}{C_z}|\vec{V}| \tag{1.27}$$

Symbol List

I	energy gradient (slope)
C_Z	Chezy Number (m½/s) (= 18 ln 4h/d_{90})
d_{90}	90 percent fractile of grain size of sediment (m)
$|\vec{V}|$	flow speed (m/s)

The second assumption is expressed through some relations between the critical friction velocity, $U_{f,crs}$ for initiation of suspension, the settling velocity, w_s and $d*$:

$$\frac{U_{f,crs}}{w_s} = \frac{4}{d_*} \quad , 1 < d_* \leq 10$$

$$\frac{U_{f,crs}}{w_s} = 0.4 \quad , \quad d_* > 10$$

(1.28)

The concentration profile is dependent upon the turbulent sediment diffusion coefficient, ε_s, and the settling velocity, w_s. In the mud transport module $\varepsilon_s = \varepsilon_f$ is assumed, where ε_f is the turbulent flow diffusion coefficient, whereas in this model the assumption is:

$$\varepsilon_s = \beta \Phi \varepsilon_f$$

(1.29)

Symbol List

β   factor, which describes the difference in the diffusion of a discrete sediment particle and the diffusion of a fluid "particle".

Φ   factor, which expresses the damping of the fluid turbulence by the sediment particles. Dependent upon local sediment concentration.

The interpretation of β is not quite clear. Some think that $\beta < 1$, because particles cannot respond fully to turbulent velocity fluctuations. However, some think that $\beta > 1$, because in the turbulent flow the centrifugal forces on the sediment particles would be greater than those on the fluid particles, thereby causing the sediment particles to be thrown to the outside of the eddies with a consequent increase in the effective mixing length and diffusion rate. In this model the following is used:

$$\beta = \begin{cases} 1 + \left(\dfrac{w_s}{U_f}\right)^2 & , \ \dfrac{w_s}{U_f} < 0.5 \\[2mm] 1 & , \ 0.5 \leq \dfrac{w_s}{U_f} < 2.5 \\[2mm] \text{no suspension} & , \ \dfrac{w_s}{U_f} \geq 2.5 \end{cases}$$

(1.30)

The Φ factor expresses the influence of the sediment particles on turbulence structure (damping effects) of the fluids.

In order to describe the concentration profile the following equation shall be solved:

$$\frac{dc}{dz} = \frac{w_s c (1-c)^5}{\varepsilon_s} \tag{1.31}$$

The determination of Φ and the solution of this equation are very time-consuming, which leads to a more simplified method, which is chosen in this model.

The distribution of the concentration profile is described by the Peclet number, P_e:

$$P_e = \frac{C_{rc}}{C_{rd}} \tag{1.32}$$

Symbol List

C_{rc}	convective Courant number (= $w_s \Delta t / h$)
C_{rd}	diffusive Courant number (= $\varepsilon_f \Delta t / h^2$)
ε_f	depth averaged fluid diffusion coefficient

This Peclet number is also called a suspension parameter, Z

$$Z = \frac{w_s}{\beta \kappa U_f} \tag{1.33}$$

Symbol List

Z	suspension parameter
κ	Von Karman's universal constant ($\kappa = 0.4$)
β	factor (as described above)

To take into account effects other than those caused by the β factor, a modified suspension parameter, Z' is defined as

$$Z' = Z + \varphi \tag{1.34}$$

where φ is an overall correction factor, which reads:

$$\varphi = 2.5 \left(\frac{w_s}{U_f}\right)^{0.8} \left(\frac{c_a}{c_o}\right)^{0.4} \tag{1.35}$$

Symbol List

c_a concentration at reference level, z = a

c_o concentration at bed, z = 0

The c_a/c_o concentration ratio is found through the following profiles:

$$\frac{c}{c_a} = \left[\frac{a(h-z)}{z(h-a)}\right]^Z \qquad \frac{z}{h} < 0.5$$

$$\frac{c}{c_a} = \left[\frac{a}{h-a}\right]^Z \exp\left(-4Z\left(\frac{z}{h}-0.5\right)\right) \quad \frac{z}{h} \geq 0{,}5 \tag{1.36}$$

c_a is based on measured and computed concentration profiles, and reads:

$$c_a = 0.015 \frac{d_{50}}{a} \frac{T^{1.5}}{d_*^{0.3}} \tag{1.37}$$

The equilibrium concentration, $\bar{c}_e$ in MIKE 21 AD equations reads:

$$\bar{c}_e = 10^6 \cdot F \cdot C_a \cdot s \tag{1.38}$$

where *F* is a relation between the bottom concentration and the mean concentration based on numerical integration of the suspended concentration profile expressed by the ratio c/c_a previously mentioned. And s the relative density equal to 2.65.

If you use a scale factor, $\bar{c}_e$ is multiplied with this factor.

Deposition is described by:

$$S_d = -(\bar{c}_e - \bar{c}) \cdot w_s^* \quad , \quad \bar{c}_e < \bar{c} \tag{1.39}$$

where w_s^* is a scaled fall velocity given by

$$w_s^* = \frac{0{,}5\,w_s}{ft} \tag{1.40}$$

Here *ft =(h*)/h*, given by equation (1.16), is the relative height of the centroid of the concentration profile. For non -uniform profiles ft is smaller than 0.5 resulting in an increase in the scaled fall velocity.

Similarly, erosion is described by:

$$S_e = -(\bar{c}_e - \bar{c}) \cdot w_s^* \ , \quad \overline{c_e} > \bar{c} \tag{1.41}$$

1.5 Bed Shear Stress

The sediment transport formulas described above apply hydrodynamic variables for describing the bed shear stress. This must be determined for pure current or a combined wave-current motion.

1.5.1 Pure currents

In the case of a pure current motion the flow resistance is caused by the roughness of the bed. The bed shear stress under a current is calculated using the standard logarithmic resistance law:

$$\tau_c = \tfrac{1}{2}\rho \ f_c V^2 \tag{1.42}$$

where

τ_c	bed shear stress (N/m²)
ρ	density of fluid (kg/m³)
f_c	current friction factor

$$f_c = 2\left(2.5\left(\ln\left(\frac{30h}{k}\right) - 1\right)\right)^{-2} \tag{1.43}$$

V	mean current velocity (m/s)
h	water depth (m)
k	bed roughness (m)

1.5.2 Pure wave motion

In the case of pure wave motion, the mean bed shear stress reads:

$$\tau_w = \tfrac{1}{2}\rho \ f_w U_b^2 \tag{1.44}$$

where

τ_w	bed shear stress
f_w	wave friction factor
U_b	horizontal mean wave orbital velocity at the bed (m/s)

$$U_b = \frac{2H_s}{T_z}\frac{1}{\sinh\left(\frac{2\pi}{L}h\right)} \tag{1.45}$$

H_s	significant wave height (m)
T_z	zero-crossing wave period (s)

An explicit approximation given by Swart (1974) for the wave friction factor is used:

$$
\begin{aligned}
f_w &= 0.47 &, \quad \frac{a}{k} < 1 \\
f_w &= \exp\left(5.213\left(\frac{a}{k}\right)^{-0.194} - 5.977\right) &, \quad 1 < \frac{a}{k} \leq 3000 \\
f_w &= 0.0076 &, \quad \frac{a}{k} > 3000
\end{aligned} \tag{1.46}
$$

where

a	horizontal mean wave orbital motion at bed (m)

$$a = \frac{H_s}{\pi}\frac{1}{\sinh\left(\frac{2\pi}{L}h\right)} \tag{1.47}$$

An explicit expression of the wave length is given by Fenton and McKee (1990):

$$L = \frac{gT_z^2}{2\pi}\left(\tanh\left[\frac{2\pi}{Tz}\sqrt{\frac{h}{g}}\right]^{3/2}\right)^{2/3} \tag{1.48}$$

1.5.3   Combined currents and waves

Three wave-current shear stress formulations are offered.

Soulsby et al

Two of the formulations use a parameterised version of Fredsøe (1984) derived by Soulsby et al. 1993.

The default option for the parameterized model is to calculate and use the mean shear stress. Another option is to calculate and use the maximum shear stress.

The mean shear stress and maximum shear stress are given by (Soulsby et al., 1993):

$$\frac{\tau_{mean}}{\tau_c + \tau_w} = \frac{\tau_c}{\tau_c + \tau_w}\left(1 + b\left(\frac{\tau_c}{\tau_c + \tau_w}\right)^p\left(1 - \frac{\tau_c}{\tau_c + \tau_w}\right)^q\right)$$

$$\frac{\tau_{max}}{\tau_c + \tau_w} = 1 + a\left(\frac{\tau_c}{\tau_c + \tau_w}\right)^m\left(1 - \frac{\tau_c}{\tau_c + \tau_w}\right)^n$$

(1.49)

where

τ_c	current alone shear stress
τ_w	wave alone shear stress amplitude
b, p, q, a, m, n	constants, which vary for different wave-current theories parameterised

For the Fredsøe (1984) model, these constants are:

$$b = b_1 + b_2|\cos\gamma|^j + (b_3 + b_4|\cos\gamma|^j)\log_{10}(r)$$

$$p = p_1 + p_2|\cos\gamma|^j + (p_3 + p_4|\cos\gamma|^j)\log_{10}(r)$$

$$q = q_1 + q_2|\cos\gamma|^j + (q_3 + q_4|\cos\gamma|^j)\log_{10}(r)$$

$$a = a_1 + a_2|\cos\gamma|^i + (q_3 + q_4|\cos\gamma|^i)\log_{10}(r)$$

$$m = m_1 + m_2|\cos\gamma|^i + (m_3 + m_4|\cos\gamma|^i)\log_{10}(r)$$

$$n = n_1 + n_2|\cos\gamma|^i + (n_3 + n_4|\cos\gamma|^i)\log_{10}(r)$$

where a_1, a_2, etc. are given in the table below, γ is the angle between waves and currents, $i = 0.8$, $j = 3.0$ and $r = 2 f_w/f_c$.

Table 1.2   Constants for wave-current shear stress formulations

	a	*m*	*n*	*b*	*p*	*q*
1	-0.06	0.67	0.75	0.29	-0.77	0.91
2	1.70	-0.29	-0.27	0.55	0.10	0.25

Table 1.2   Constants for wave-current shear stress formulations

	a	m	n	b	p	q
3	-0.29	0.09	0.11	-0.10	0.27	0.50
4	0.29	0.42	-0.02	-0.14	0.14	0.45

Fredsøe

A third option is to calculate and use the bed shear stress found from Fredsøe (1981).

The effect on the outer current velocity profile is described by introducing a "wave" roughness, k_w, which is larger than the actual bed roughness.

It is assumed that the wave motion is dominant close to the bed compared to the current, which means that the wave boundary layer thickness, δ_w, and wave friction, f_w, can be determined by considering the wave parameters only. The wave boundary thickness, δ_w, is found by (Johnsson and Carlsen, 1976):

$$\delta_w = 0{,}072 k \left(\frac{a}{k}\right)^{0{,}75}$$ (1.50)

where k is bed roughness and a defined by eq. (1.47).

The velocity profile outside the wave boundary layer, which is influenced by the wave boundary layer is given by

$$\frac{U(z)}{U_{fc}} = 2{,}5 \cdot \ln\left(\frac{30z}{k_w}\right)$$ (1.51)

where

U(z)	velocity at vertical coordinate *z* (m/s)
Ufc	friction velocity (m/s)
k_w	wave roughness (m)

In case of weak wave motion, where the wave roughness *kw* is less than the bed roughness *k* for pure current motion, the latter will be used.

The mean bed shear stress for combined wave-current motion is given by

$$\tau_b = \frac{1}{2}\rho f_w (U_b^2 + U_\delta^2 + 2 U_b U_\delta \cos\alpha)$$ (1.52)

where

U_d	current velocity at top ($z=\delta$) of wave boundary layer (m/s)
α	angle between the mean current and the direction of wave propagation

The resulting bed shear stress is found as the largest value of the bed shear stress for pure current, derived by eq. (1.42), and the value derived by eq. (1.52).

1.6 Multi-layer and multi-fraction applications

The MT model is a multi-layer and multi-fraction model. In the water column the mass concentrations c_1, c_2, etc. to c_i are defined. In the bed $c_{1,1}$, $c_{2,1}$, etc. to $c_{i,1}$ are defined for the first layer and $c_{1,2}$ $c_{2,2}$, etc. to $c_{i,2}$ for the second layer and consecutively. See also Figure 1.5.

Figure 1.5   Definition sketch for multi fractions-layers

The fractions are defined by their sediment characteristics. For the cohesive sediment fractions this gives the following extensions to the formulae above for deposition and erosion.

The deposition for the *i* mud fraction is:

$$D^i = w_s^i c_b^i p_D^i \tag{1.53}$$

where p_D^i is a probability ramp function of deposition:

$$\upsilon_D^i = max\left(0, min\left(1,1 - \frac{\tau_b}{\tau_{cd}^i}\right)\right) \tag{1.54}$$

Erosion of the top layer of the bed is considered one incident calculated for one time step updating the sediment fraction ratio of the bed.

In the MT module, the sand transport description is based on the assumption that erosion takes place simultaneously for both sand and cohesive sediment. Therefore, the erosion of each layer is calculated using the normal mud transport erosion equations. Afterwards, the fraction of the sediment that may be kept in suspension under the present hydrodynamic conditions is calculated.

Thus, for a dense consolidated bed the erosion rate from the top layer j, can be calculated in the following way:

$$E_{j,\,total} = E_0^j \, p_E^{j\,E_m} \tag{1.55}$$

where p_E^i is a probability ramp function of erosion and E_0 is the erodibility.

$$p_E^j = max\left(0, \frac{\tau_b}{\tau_{ce}^j} - 1\right) \tag{1.56}$$

The erosion rate for the fraction *i* is then calculated as:

$$E_{i,j} = \frac{M_{i,j}}{M_{total,j}} E_{total}^i \tag{1.57}$$

In which *M* is the mass of sediment in the layer *j*.

Similarly for a soft, partly consolidated bed:

$$E_{j,\,total} = E_0^j \exp(\alpha^j (\tau_b - \tau_{ce}^j)^{0.5}) \tag{1.58}$$

The erosion rate for the fraction *i* is then calculated as:

$$E_{i,j} = \frac{M_{i,j}}{M_{total,j}} E_{total}^i \tag{1.59}$$

Each layer in the bed contains a certain concentration of sediment defined by a dry density excluding water content. This density is assigned the set of fractions applied. For example 60 percent particles < 63 μm and 40 percent fine

sand. This ratio is not fixed but can vary throughout the simulations, dependent on the advection-dispersion processes. An account is kept of the sediment ratios for the bed. This allows for a grain sorting process to take place.

1.7 Morphological Features

1.7.1 Morphological simulations

The morphological evolution is sought to be included by updating the bathymetry for every timestep with the net sedimentation rate. This ensures a stable evolution in the model that will not destabilise the hydrodynamic simulation.

$$Bat^{n+1} = bat^n + netsed^n \tag{1.60}$$

where:

bat_n	Bathymetry at present timestep
bat_{n+1}	Bathymetry at next timestep
n	Timestep

The MT module also allows the morphological evolution to be speeded up in the following way.

$$Bat^{n+1} = bat^n + netsed^n \, Speedup \tag{1.61}$$

Speedup is a dimensionless factor. This factor is relevant for cases where the sedimentation processes are governed by cyclic events such as tides or seasonal variation. This does NOT apply to stochastic events such as storms.

The thickness of the individual bed layers is updated at the same time as the bathymetry. This is not the case for the suspended concentration.

1.7.2 Bed update

The bed layer is updated using the following logistics (only 1 layer and 1 fraction is considered)

The net deposition is calculated as $ND = \sum_I (D^i - E^i)\Delta t$

The bed mass M is calculated.

If net erosion occurs (ND > 0) and M + ND < 0, the deposition and erosion rates are adjusted such that M + ND = 0.

The bed layer thickness and density are updated as

$$H_{bed}^{new} = H_{bed}^{old} + \frac{ND \cdot \Delta t}{\rho^i} for\ ND > 0$$

$$H_{bed}^{new} = H_{bed}^{old} + \frac{ND \cdot \Delta t}{\rho_{bed}^{old}} for\ ND > 0$$

$$\rho_{bed}^{new} = \frac{H_{bed}^{old} \cdot \rho_{bed}^{old} + ND \cdot \Delta t}{H_{bed}^{new}}$$

(1.62)

1.8 Data Requirements

Bathymetry and Hydrodynamics

Wave Input
- Mean wave heights
- Mean wave periods
- Mean wave directions

Calibration Factors
- Dispersion coefficients
- Critical shear stress for deposition for each fraction
- Erosion coefficient
- Power of erosion
- Transition coefficient
- Sliding coefficient
- Bed roughness

Sediment Input
- Settling velocity for each fraction
- Flocculation parameters
- Dry densities of each fraction
- Critical shear stress for erosion

Initial Conditions
- Initial thickness of bed layers
- Initial concentration of suspended sediment
- Initial grain size distribution of the bed

Boundary Conditions
- Suspended sediment concentrations

Morphology
- Speedup factor

1.9 List of References

Andersen, T.J. 2001.
Seasonal variation in erodibility of two temperate microtidal mudflats. Estuarine, Coastal and Shelf Science 56, pp 35-46

Andersen, T.J. & Pejrup, M. 2001.
Suspended sediment transport on a temperate, microtidal mudflat, the Danish Wadden Sea. Marine Geology 173, pp 69-85

Burt, T.N. 1986.
Field settling velocities of estuary muds. In *Estuarine Cohesive Sediment Dynamics. Lecture Notes on Coastal and Estuarine Studies*. (Mehta, A.J., ed.). Springer Verlag, Berlin, pp 126-150.

Delo, E.A., Ockenden, M.C.
"Estuarine Muds Manual" HR Wallingford, Report SR309, May 1992.

Dyer, K.R. 1986.
Coastal and Estuarine Sediment Dynamics. John Wiles & Sons, pp 342

Edelvang, K. & Austen, I. 1997.
The temporal variation of flocs and fecal pellets in a tidal channel. Estuarine, Coastal and Shelf Science 44, 361-367.

Eisma, D. 1993
Suspended matter in the aquatic environment. Springer Verlag, pp 315

Ekebjærg, L. and Justesen, P.
"An Explicit Scheme for Advection-Diffusion Modelling in Two Dimensions". Comp. Meth. App. Mech. Eng., 1991, pp. 287-297.

Engelund, F., Fredsøe, J.
"A sediment transport model for straight alluvial channels". Nordic Hydrology 7, 1976, pp. 293 - 306.

Fenton and McKee
"On Calculating the Lengths of Water Waves". Coastal Engineering, Vol. 14, Elsevier Science Publishers BV, Amsterdam, 1990, pp. 499-513.

Fredsøe, J.
"Mean Current Velocity Distribution in Combined Waves and Current". Progress Report No. 53, ISVA, Technical University of Denmark (1981).

Fredsøe, J.
"Turbulent boundary layer in wave-current motion". J Hydr Eng, A S C E, Vol 110, HY8, 1103-1120 (1984).

Gibbs, R.J. 1985
Estuarine flocs: Their size, settling velocity and density. Journal of Geophysical Research 90, pp 3249-3251

Grishanin, K.V, and Lavygin, A.M.
"Sedimentation of dredging cuts in sand bottom rivers". PIANC, Bulletin 1987, No. 59, pp. 50-55.

Jonsson, I.G. and Carlsen, N.A.
"Experimental and Theoretical Investigations in an Oscillatory Rough Turbulent Boundary Layer". J. Hydr. Res. Vol. 14, No. 1, pp. 45-60 (1976).

Krone, R.B.
"Flume Studies of the Transport of Sediment in Estuarial Processes". Hydraulic Engineering Laboratory and Sanitary Engineering Research Laboratory, Univ. of California, Berkely, California, Final Report, (1962).

Krone, B. 1986
The significance of aggregate properties to transport processes. In: Mehta A.J. (Ed) Estuarine Cohesive Sediment Dynamics, Springer Verlag, p 66-84

Leonard, B.P.
"A stable and accurate convective modelling procedure based on quadratic upstream interpolation". Comput. Meths. Appl. Mech. Eng. 19 (1979), 59-98.

Leonard, B.P.
"The ULTIMATE Conservative Differential Scheme Applied to Unsteady One-Dimensional Advection". Comput. Meths. Appl. Mech. Eng. 88 (1991), 17-74.

Mehta, A.J., Hayter, E.J., Parker, W.R., Krone, R.B., Teeter, A.M.
"Cohesive Sediment Transport. I: Process Description". Journal of Hydraulic Eng., Vol. 115, No. 8, Aug. 1989, pp. 1076-1093.

Pejrup, M. 1988a.
Flocculated suspended sediment in a micro-tidal environment. Sedimentary Geology 57, 249-256.

Pejrup, M., Larsen, M. and Edelvang, K. 1997.
A fine-grained sediment budget for the Sylt-Rømø tidal basin. Helgoländer Meeresuntersuchungen 51, 1-15.

Postma, H. 1967
"Sediment Transport and Sedimentation in the Estuarine Environment". In: Lauff G.H: (Ed) Estuaries AAAS Publ. 83, p 158-179

Rijn, L.C.
"Sediment Transport, Part I Bed Load Transport". Journal of Hydraulic Engineering, Vol. 110, No. 10, October, 1984.

Rijn, L.C.
"Sediment Transport, Part II Suspended Load Transport". Journal of Hydraulic Engineering, Vol. 110, No. 10, October, 1984.

Rijn, Van L.C.
"Handbook on Sediment Transport by Current and Waves". Delft Hydraulics, Report H461, June 1989, pp. 12.1-12.27.

Soulsby RL, Hamm L, Klopman G, Myrhaug D, Simons RR, and Thomas GP.
"Wave-current interaction within and outside the bottom boundary layer".
Coastal Engineering, 21, 41-69 (1993).

Swart, D.H.
"Offshore sediment transport and equilibrium beach profiles". Delft Hydr. Lab. Publ., 1312, Delft Univ. technology Diss., Delft, 1974.

Teeter, A.M.
"Vertical Transport in Fine-Grained Suspension and Nearly-Deposited Sediment". Estuarine Cohesive Sediment Dynamics, Lecture Notes on Coastal and Estuarine Studies, 14, Springer Verlag, pp. 126-149 (1986).

Teisson, C.
"Cohesive suspended sediment transport: feasibility and limitations of numerical modelling". Journal of Hydraulic Research, Vol. 29, No. 6, 1991.

Van Leussen, W. 1988.
Aggregation of particles, settling velocity of mud flocs. A review: In: Dronkers & Van Leussen (Eds.): Physical processes in estuaries. Springer Verlag, pp 347-403.

Van Olphen, H. 1963
"An introduction to clay colloid chemistry. ". Interscience Publishers (John Wiley & Sons) pp 301.

Whitehouse, U.G., Jeffrey, L.M., Debbrecht, J.D. 1960
Differential settling tendencies of clay minerals in saline waters. In: Swineford (Ed) Clays and clay minerals. Proceedings 7th National Conference, Pergamon Press, p 1-79.

Yalin, M.S
"Mechanics of Sediment Transport". Pergamon Press Ltd. Hendington Hill Hall, Oxford, 1972.

INDEX